

Received April 13, 2021, accepted May 11, 2021, date of publication May 17, 2021, date of current version May 25, 2021.

Digital Object Identifier 10.1109/ACCESS.2021.3081457

# Intelligent Blowgun Game Scoring Recognition System Based on Computer Vision

SHIH-CHANG HSIA<sup>1</sup>, SZU-HONG WANG, WEI-CHUN CHENG,  
AND CHUAN-YU CHANG<sup>1</sup>, (Senior Member, IEEE)

Department of Electronics Engineering, National Yunlin University of Science and Technology, Douliou 64002, Taiwan

Corresponding author: Shih-Chang Hsia (hsia@yuntech.edu.tw)

This work was supported by the Intelligent Recognition Industry Service Center from The Featured Areas Research Center Program within the framework of the Higher Education Sprout Project by the Ministry of Education (MOE), Taiwan.

**ABSTRACT** In this manuscript, we present score recognition techniques for blowgun game based on computer vision. First, the algorithm detects the position of the target, and calibrates the camera's parameters. Then the score is calculated with the detection of the dart tip on the target for real-time applications. To improve the robustness, the initial calibration is proposed to record N points as references at the edges of circles, to correct the camera position and angle. This approach can overcome the problems of lighting changes and the camera viewing angle deviation. The fast segmentation and orientation decision is proposed to find the blowgun tip accurately. The two cameras are presented to solve the overlapping problem of multiple darts to improve the detection accuracy. Based on calibration parameters, the distance weighting method is proposed to calculate the score precisely. Experiments result that the accuracy can achieve about 97% to recognize the score, and the processing speed can meet the real-time requirement with software implementation.

**INDEX TERMS** Segmentation, localization, blowgun game, score, recognition.

## I. INTRODUCTION

Recently, the computer vision is a new technology, which can provide more convenient applications for users. Imaging recognition is the key technology in vision for various applications. Now, many systems proposed employ computer vision technology. For security system, iris recognition used biometric identification for human authorized [1]. Human face detection can localize face position, and the recognition algorithm compares with the selected facial features and a facial database, to find user information promptly [2]. Text detection and recognition is to find text information from an image, which can be applied for machine learning and video index search [3]. The applications of computer vision are more and more now, even for animal health care and animal classification [4]. The traffic sign detection and recognition [5], and car license plate recognition [6], [7] are proposed for intelligent transportation systems. The dynamic hand gesture recognition for computer understanding is presented in [8], which can use gesture to control various operations through camera device.

The associate editor coordinating the review of this manuscript and approving it for publication was Diego Oliva<sup>1</sup>.

In this study, a new application for the sport scoring system is proposed by image recognition based on computer vision. Archery is originated in ancient military and sport activities. Currently, archery has turn out to be an internationally sports, such as Olympic Games and World Games. Similarly, blowgun system were used, which recorded by people since 1519 in France and 1688 in Japan. Until now, there are some tribal hunters also used blowguns to hunt animals. The principle is the gas pressure difference across the arrow and produces a forward force. Recently, the blowgun is a popular sport in Japan [9]. The blowgun system consists of one blowpipe, five arrows and one target board. The blowpipe is made of carbon fiber or glass fiber and its length is about 120cm. When the human blows the arrow through blowpipe to the target, the score is calculated by the accumulation of each dart score after five times. Currently, the score must be recorded by human power. It is inevitable argument when the arrow falls at the margin of between two scores. The computer vision can take fair judgment at the margins to avoid the argument.

The automatic dart-scoring system is a challenge work. Recently, the automatic target-scoring systems are presented with camera imaging methods [23]–[28]. The automatic

bullet scoring system is presented for military training [23], which employs geometric rectification and the median filter, image binary, image subtraction between inter-frames to find the position of bullet-spot. Automatic display system of the archery score is presented in [24], which used boundary line detection and arrow detection to determine the score. Effective target area [25] is detected using edge extraction and background extraction, and then perspective transformation. The scoring target for mobile shooting range detection employs external vibration sensing, and the morphological operation detects the effective outermost ring, finally SVM is used to find discriminating bullet hole candidates [26]. The detection method uses the morphological operations, segmentation by using color and shape features [27], which adopts dynamic threshold to reduce the effects of illumination changing.

Our motivation is to develop a score recognition system using computer vision technology to make fair judgment, particularly for margin point. By using the way, the users can immediately know the score of current dart from the far distance. The computer can accumulate the score for each competitor and show the competition rankings from database automatically. In this paper, the target localization and segmentation are proposed to find the dart tip. The initial calibration is presented to reduce the affection of camera angle deviation and the light changing. The double cameras are adopted to overcome the overlapping problem and improve the accuracy. The rest of this paper is organized as follows. The target localization and data calibration is proposed in Section II. The automatic score recognition is presented in Section III. The real-time implementation and experiments are described in Section IV. The conclusions are marked in Section V.

**II. PROPOSED LOCALIZATION AND CALIBRATION ALGORITHM**

In a free space, first the scoring systems must detect the position of target accurately. To reduce the camera noise, the median filter first is used to suppress the noise level. Then the pre-processing with de-flicker and white-balance is required [10], [11], to improve the video quality. In order to not interfere with users playing the game, the camera should be setup from the far distance to the target. Hence the background of target would be included at the image sampling. For score recognition, we must detect the target location and remove the background as well. Figure 1(a) and (b) show the original gray image and its result using edge detection by Sobel mask [12], respectively. The edges of score circles are clearly exposed. The circle detection is used to localize the position of target [13], [14].

**A. CENTER POINT DETECTION**

The accurate localization for the target board is important for scores computing. The score circles in Fig. 1(b) are detected by circle detection. Only circle information is kept for the processing. The central point is a basis reference

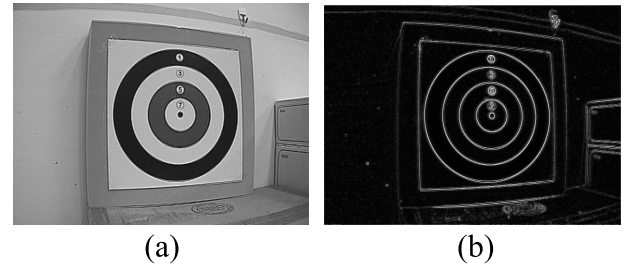


**FIGURE 1. The target localization, (a) and (b) the original Y image and edge detection using Sobel mask respectively.**

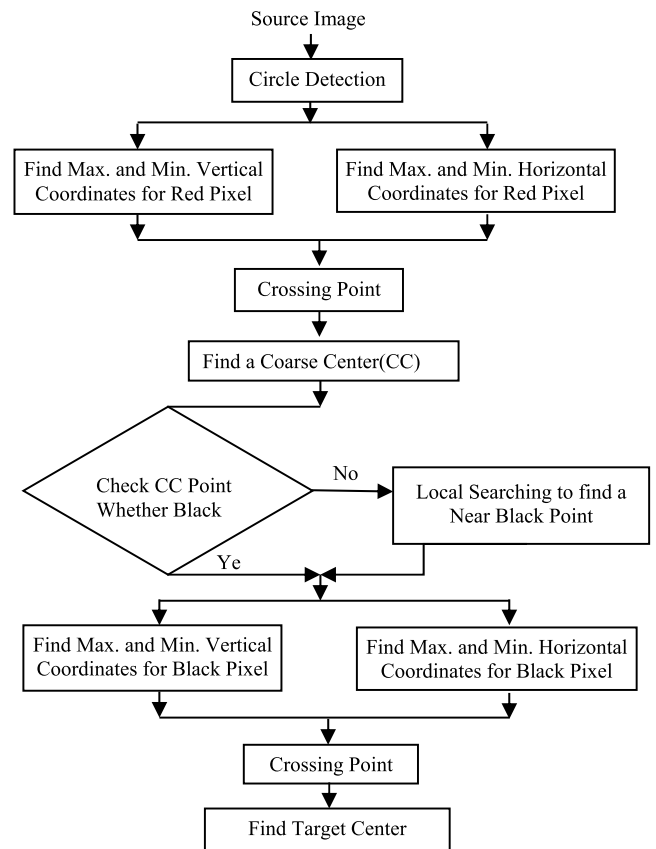


**FIGURE 2. The proposed center detection on target paper.**

point for the score calculation. This point must be localized accurately, to avoid the score deviation. The central point of circles from on the target board is searched fast, as shown in figure 2. First, the inner circles are detected. Then the minimum and maximum value of horizontal coordinates are searched with the names  $(X1,Y)$  and  $(X2,Y)$  respectively, as shown in Fig. 3(a). Also, the maximum and minimum value of vertical coordinates are found with  $(X,Y1)$  and  $(X,Y2)$ . The pixels  $(X1,Y)$  and  $(X2,Y)$  is connected as a horizontal line HL. By similar method, one can connect  $(X,Y1)$  to  $(X,Y2)$  as a vertical line VL. Then HL and VL lines can be crossed to one point that is called a coarse center (CC) point. If CC is a black point, this point is a central point. Otherwise, when CC is not a black point, a local searching approach is used to find a black point from the current CC within a block size. To localize the center point accurately, the maximum and minimum vertical/horizontal coordinates on the central black

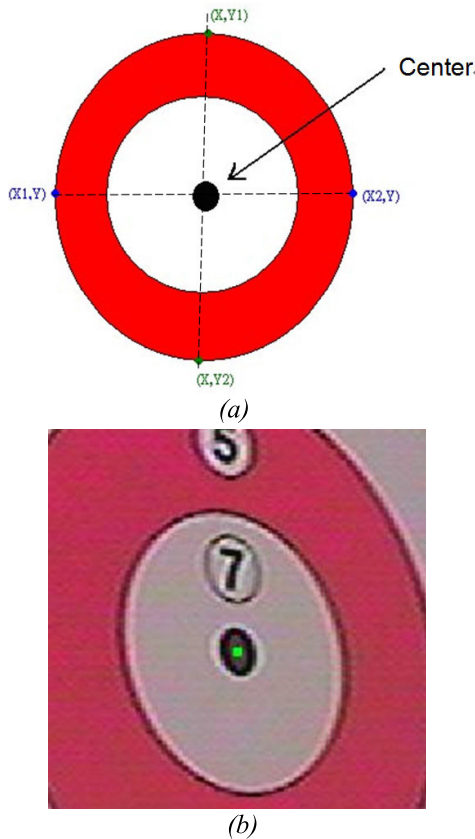


**FIGURE 3.** The detection of center point. (a)The max. and min. value at vertical and horizontal coordinates. (b)The center point of circle found accurately.

point are searched again. Similar to the previous mentioned, the two lines are crossed by a point that is the accurate center of target. Figure 3(b) shows the central point of circle marked with high precision by using the intersection of horizontal and vertical lines across the target paper to overcome the problem of angle deviation from camera.

## B. INITIAL CALIBRATION

The camera is setup at various directions and angle in a practical system. Because the target is not perfectly circular sampled, the radius around one target ring is not constant. The deviation of each direction must be calibrated to improve the detection accuracy. First the system is calibrated to record the new data for the current camera setup situations to promote the robustness. Initially, the system is calibrated using the distance parameters from the central point to the calibrated point on multi circle edges under difference directions. This can improve the system robustness when the background brightness changes or target moves. To estimate the dart score, the distance of circle radius is measured. The radius from the central-point to each circle must be calibrated. Due to camera viewing angles, the distance from the center point to each circle is different on various directions. The initial calibration is proposed to correct this deviation to improve the accuracy. The circle scores are split with 8 directions, by using  $0^\circ, 45^\circ, 90^\circ, 135^\circ, 180^\circ, 225^\circ, 270^\circ, 315^\circ$ , as shown

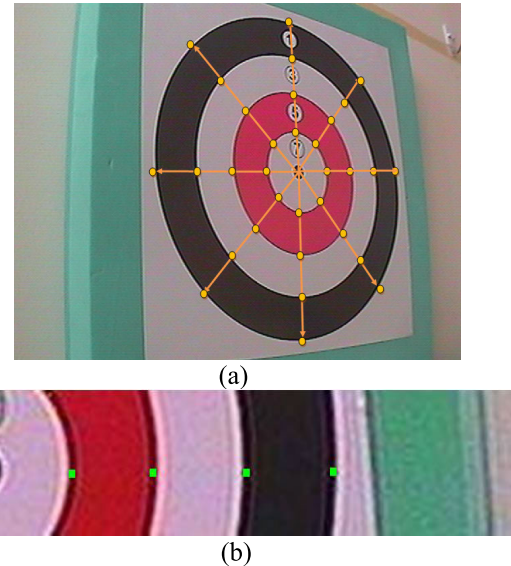


**FIGURE 4.** The detection of calibration point (a)The 8 directions for each circle scores marked; (b)The precision dark point found between two color boundaries.

in Figure 4(a). The distance is calculated from the center point to the circle edge of each direction, which can be expressed by

$$Dist_n^{Deg} = \sqrt{(Center(x) - Score_n^{Deg}(x))^2 + (Center(y) - Score_n^{Deg}(y))^2}, \quad (1)$$

where  $Center(x)$  and  $Center(y)$  is the coordinates of center point,  $Score_n^{Deg}(x)$  and  $Score_n^{Deg}(y)$  denotes the  $(x,y)$  coordinates of the directional degree at the  $n$ th circle edge.  $Dist_n^{Deg}$  is the distance from the  $n$ th circle to the center point at the Deg direction. For score computing, the distances from each circle to the central point are measured from each direction. One direction angle has four circle radiuses, which are recorded for score estimation later. In the initial calibration step, 32 radiuses are calculated from the detection of four circles with eight directions. Due to viewing angle, the circle radiuses are difference in each direction. The 32 radiuses must be stored for data calibration before user shooting.

Figure 5 shows the flowchart for computing distance of the calibrated points on each circle. To recognize the score of each circle on target automatically, the distance from the center point to each circle must be calibrated first. The circles can be detected rough by using edge detection, which is further quantified to binary and then to segment the circles. Now some pixels after edge detection are not continuous. A  $3 \times 3$  closing operation [12] is used to recover the circle edge information. However, the position of circle point using edge detection is not precise. This will degrade the accuracy of score recognition. In order to improve the accuracy, the circle point from edge detection is further mapping to the original RGB color image. When enlarging the image for color circles, the darkest point on the circle can be found due to the boundary effect between two colors, as shown in Fig. 4(b) [15], [16]. This darkest point can be used to calculate the

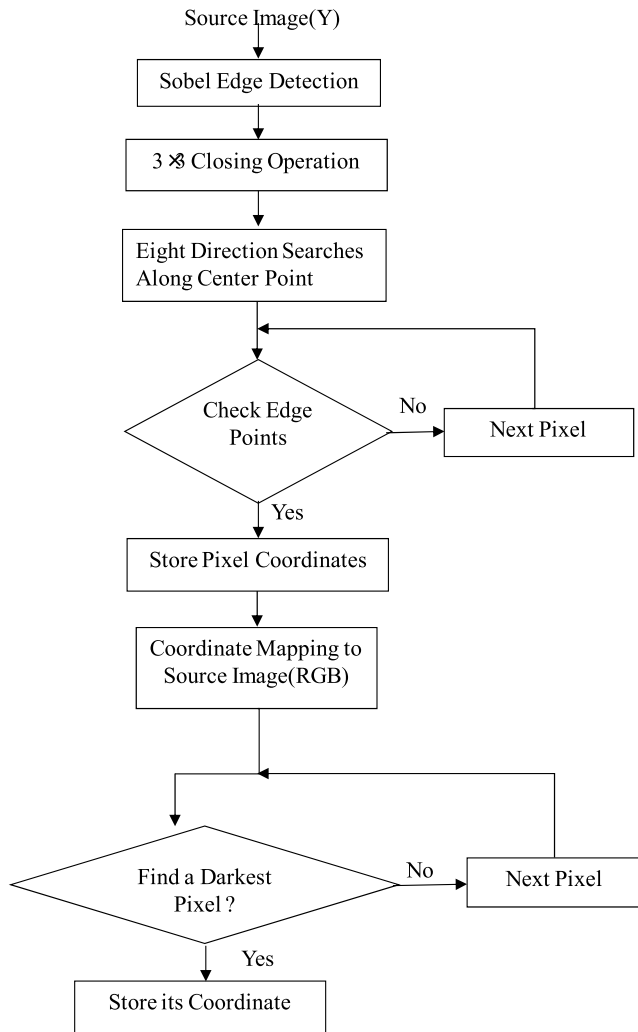


FIGURE 5. The processing of distance calibration for each circle.

circle radius accurately, which can be searched with local region searching. The results are shown in Fig. 4(b) that can be detected in high accuracy. The calibration data is measured with eight directions. After calibration, the stored parameters include the relative 32 coordinates and its distance.

Alternatively, the other method is to map the target image to a front-on plane using ellipse fitting model [29]. However, we must create many ellipse models to map which one is suitable in the current camera sampling angle. This method must be one-by-one mapping the current data to the training model with the training data. The processing time will become long. If the mapping model is not perfect to the camera, the score estimation will appear errors.

III. PROPOSED SCORE RECOGNITION ALGORITHM

For score recognition, first the dart is detected soon whether enter to the target board. Figure 6 shows the processing flowchart to find the new dart based on object segmentation [17], [18]. The dart is a moving object that can be segmented from each shooting. When a new dart enters to the target board, the temporal differential between the current frame

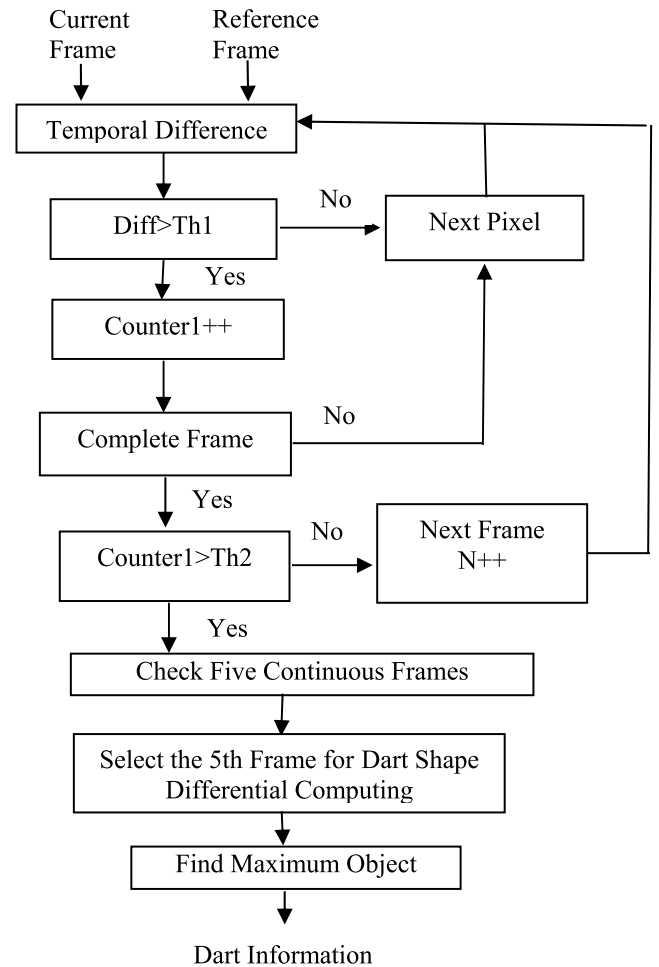


FIGURE 6. The processing flowchart for the new dart detection.

and the reference frame become high. The amount of differential value is calculated to estimate whether the dart coming now. When the frame size is  $N \times M$ , the absolute difference of each pixel  $Diff(x,y)$  is calculated by

$$Diff(x,y) = |Ref(x,y) - Current(x,y)|, \text{ for } x = 1 \text{ to } N, y = 1 \text{ to } M. \quad (2)$$

where  $Ref(x,y)$  and  $Current(x,y)$ , is the reference pixel and the current pixel at the  $(x,y)$  coordinate, respectively. If  $Diff(x,y)$  is larger than the threshold  $Th1$ , the counter1 is increased by one. The counting is finished until all pixels are checked.  $Th1$  is used to check the difference of the temporal frames whether satisfied. If the  $Th1$  is too low, the noise will interfere with the detection accuracy. The level of camera noise between inter-frames always is less than 18. The  $Th1$  takes 20 in experiments. When one frame is done, the new dart is found if the amount of counter1 is over than the threshold  $Th2$ . Otherwise, the new dart information is not found at the current frame. The next frame is checked and the counter1 is reset to zero until a new dart is found.  $Th2$  is used to check whether the new dart shooting. Generally, the dart image includes at least 40 pixels. If  $Th2$  is set too high, the probability of the missing detection for darts would increase. The threshold  $Th2$  is set to 42 in experiments. Five

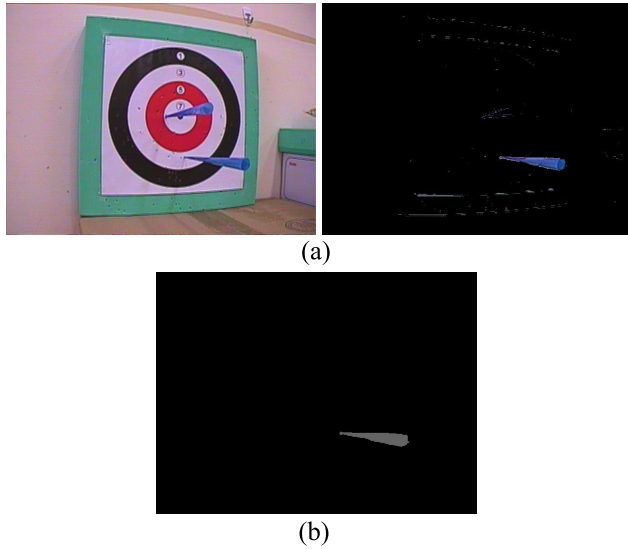


FIGURE 7. The detection of dart. (a) The differential information for the second dart. (b) The segmentation of the second dart shape.

consecutive frames are checked to make sure the dart shooting on the target already. If the dart information appears on five consecutive frames, the new dart shooting on the target paper can be confirmed now. When the dart is confirmed at the  $N^{th}$  frame, the image sampling for the next  $(N+1)^{th} \sim (N+3)^{th}$  frames may be not stable because the current dart is running now. To sample the dart image stably, the  $(N+4)^{th}$  frame is adopted for the processing. When the new dart is detected, the dart shape is calculated with the absolute subtraction with the reference frame. Figure 7(a) shows the original frame and the differential pixel for the second dart. When the dart impacts the target, the target paper slightly wobbles, and noisy pixels appear. To solve this problem, maximum object tracking is used to find the dart location since the dart shape is a maximum object. To reduce the problem about the horizontal and vertical gradients of a dart, the dart is truncated to binary. The result is shown in Fig. 7(b), where the background pixels all are truncated to zeros. When the new dart shape is found, the reference frame is updated by the current frame for the next new dart is checked. In order to reduce the lighting affect, the reference frame is automatically updated per second if no dart is detected.

When the dart shape is found, the score of the current dart is calculated according to its position. Figure 8 shows the processing flow of the dart score computing. The dart orientation and its tip must be detected accurately. If the dart direction is horizontal, its tip will be either right or left. Otherwise, the dart direction is vertical, where its tip will be either up or bottom. The dart direction is determined by histogram distribution of horizontal and vertical direction, as shown in Fig. 9. The histogram-based method only uses counters to record the coordinate distribution for the dart shape. The computations are not high. The number of horizontal shape for the dart is counted by width (W) pixels. Fig. 10(a) shows the horizontal histogram of Fig. 7(b), the coordinate distribution is 365~505. The histogram range for the horizontal shape

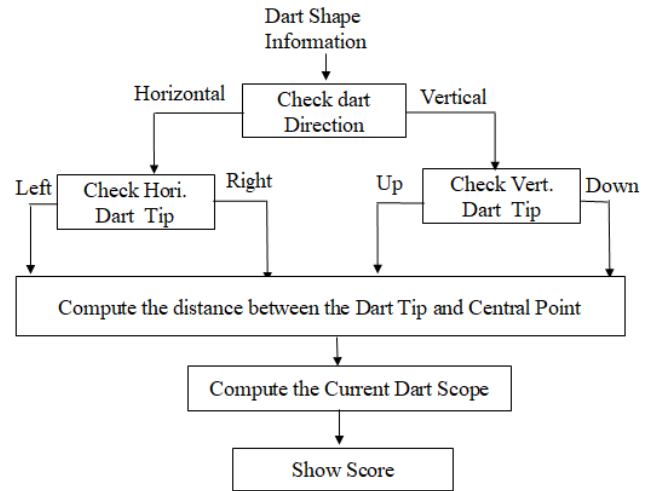


FIGURE 8. The flowchart of the dart score computing.

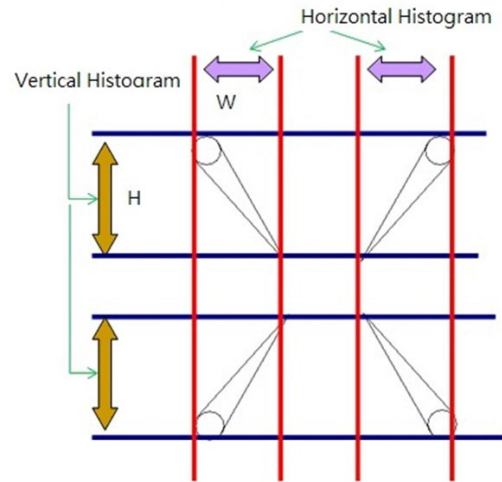


FIGURE 9. The dart direction checking by histogram.

is defined by  $\Delta W = W1 - W2 = 505 - 365 = 140$ , where  $W1$  and  $W2$  is the start and end of horizontal coordinate in histogram respectively. Similarly, the vertical histogram calculates the height (H) of the dart shape, as shown in Fig. 10(b). The coordinate distribution is 325~343. The histogram range for the dart shape in the vertical direction is  $\Delta V = V1 - V2 = 343 - 325 = 18$ , where  $V1$  and  $V2$  is the start and end of vertical coordinate in histogram respectively. If  $\Delta W > \Delta V$ , the dart belongs to the horizontal direction; otherwise, it is vertical. Clearly, the Figure 7(b) is a horizontal dart since  $\Delta W > \Delta V$ .

To detect the dart tip, there are four cases, as shown in Fig. 11 (a)~(d). When the dart direction is horizontal, the scanning direction is from the left to the right. The dart coordinate of the first and final point is symbolized as  $J\_Lfirst$  and  $J\_Lfinal$  respectively, and the maximum coordinate in histogram is  $J\_max$ . If  $|J\_Lfinal - J\_max| > |J\_Lfirst - J\_max|$ , the dart tip locates at the right side. as shown in Fig. 11(a). Otherwise, it is at the left side, as shown in Fig. 11(b). Clearly, the dart tip in Figure 7(b) is at the left side since  $|J\_Lfinal - J\_max| < |J\_Lfirst - J\_max|$ . Similarly, when the dart direction is vertical, the scanning direction is from up to down. The first and final coordinates are symbolized as

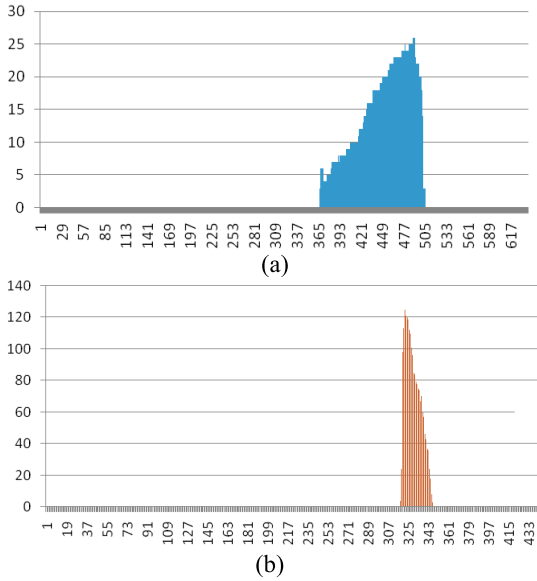


FIGURE 10. Dart histogram.(a)The dart horizontal histogram of Fig. 7(b); (b) The dart vertical histogram of Fig. 7(b).

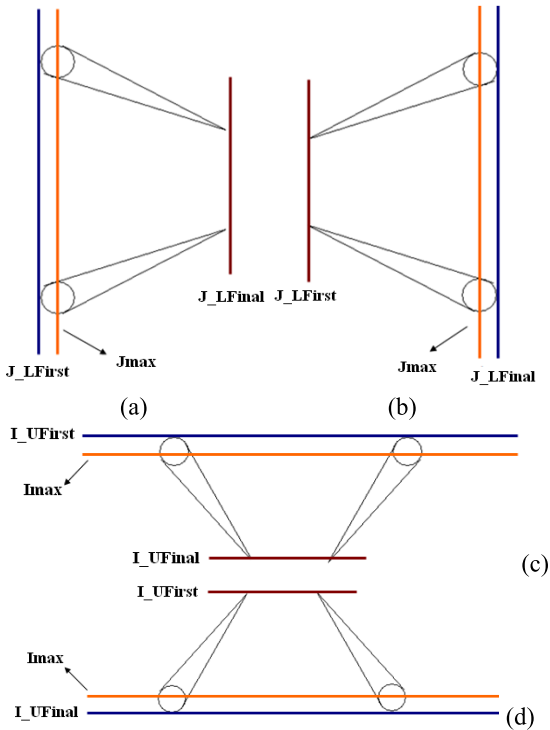


FIGURE 11. (a) -(d) The dart tip located at the right, left, bottom and top respectively.

I\_Ufirst and I\_Ufinal, respectively. The maximum coordinate in histogram is I\_max. If  $|I\_Ufinal - I\_max| > |I\_Ufirst - I\_max|$ , the dart tip locates at the bottom side, as shown in Fig. 11(c). Otherwise, the tip is at the up direction, as shown in Fig. 11(d).

The scoring accuracy depends on the tip segmentation of the newly detected dart. The dart tip may get shorten about 1~2 pixels after segmentation, which will slightly effect the detected accuracy. The  $3 \times 3$  dilate operation is used to expand the tip area to trim the accuracy in practical measurements.



FIGURE 12. The segemation of dart tip detected accuracy.

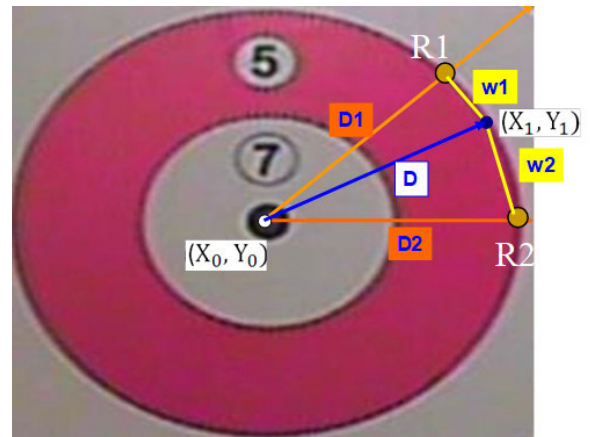


FIGURE 13. The distance computing between the central point and dart tip.

While the dart direction is decided, the tip point can be found by the first pixel of the specified direction. Figure 12 shows the dart tip marked. The final score is decided by the distance between the dart tip and the central point. Figure 13 illustrates the distance computation for the current dart. The distance is calculated by

$$Dart\_Dist = \sqrt{(Dart(X_1) - Center(X_0))^2 + (Dart(Y_1) - Center(Y_0))^2}, \quad (3)$$

where  $Dart(X_1)$  and  $Dart(Y_1)$  denotes the coordinates of the current dart tip.  $Dart\_Dist$  in (3) calculates the distance from the dart tip to the central point. The distance and its coordinates of each circle degree had been pre-recorded as parameters on the memory during calibration period. First, the coordinates of two calibrated points R1 and R2 close to the current dart tip are searched. From Figure 13, D1 and D2 denote the pre-recorded distances from the points R1 and R2 to the central point respectively. The weight distance is proposed to calculate the score accurately. The estimated score distance (ESD) is calculated by

$$ESD = \frac{D_1 \times W_2 + D_2 \times W_1}{W_1 + W_2}, \quad (4)$$

where W1 and W2 is the distance from the recorded points R1 and R2 to the dart tip respectively. The estimated score

distance (ESD) in (4) calculates the distance from the dart tip to the calibrated point with  $W_1, W_2$  weights of  $R_1$  and  $R_2$ . If the tip is close to the point  $R_1$ , the weight for  $D_1$  is increased to correct the degree error from the camera. Since the calibration uses the 8 directions, the angle of  $D_1$  and  $D_2$  relative to the tip position is less than 23 degree. The estimated error is small. For higher accuracy, the more directions can be employed, but the computational time would increase. With (4), if  $W_2 > W_1$ , the weight of  $D_1$  is enhanced by  $W_2 / (W_1 + W_2)$  since the current dart is closer to  $R_1$ . The parameters  $D_1, D_2, W_1$  and  $W_2$  are adaptive dependent on the position of camera and the dart tip location. Now the dart score can be decided by comparison with ESD and Dart\_Dist. If the  $ESD > \text{Dart\_Dist}$ , the current dart is closer center than the calibrated point, so the score is inside circle. Otherwise, it is the outside circle. For example, the score of the outside circle is 3, and the inside is 5, in Fig. 13.

It is worthy notice that the darts may be overlapped since there are five darts at one game. This will impact the detection accuracy. To overcome the overlapping problem of multi darts, two cameras are proposed to solve this problem. The two cameras are setup at the inverse location to compensate the errors each other. Each camera samples the image with analog to digital converter (ADC) at the same time, then the imaging pixels are processed with the same processing procedure. In fact, the darts on the target are random. The dart is segmented to find its tip and then to measure the score. If the darts are overlapping each other, its tip is possibly masked and its score will be down. When the right camera happens overlapped and the left camera is normal, in such a case, the score of left camera is adopted. For fast processing, the maximum score of two cameras is selected as for the results, since the low scoring camera would occur at the problem of darts overlapping. This method can effectively reduce the affection of overlapping, and avoid wasting on the high computing power on the detection of overlapping images. The complex multi-view algorithm can be used to solve the overlapping problem more effectively. However, the complexity of this kind algorithm is very high, which will impact the real-time speed. The hardware acceleration must be considered to improve the processing speed. The current version takes the maximum value operation for real-time processing requirement. This approach achieves enough accuracy for real applications.

#### IV. EXPERIMENTS

For practical test, the automatic scoring system for blowgun game is setup, as shown in Figure 14. All equipments are following to the standard of Sport Fukiya Association in [9]. In order to correct the dart overlapping error, two cameras are positioned on the left side and the right side respectively, which samples the target images by the inverse direction. Then the sampling image is digitalized with  $640 \times 480$  pixels by a catch card DVP-7010BE [20]. The sampling data is sent to a computer for score computing on real-time processing. Based on our algorithm, C-programming is performed to



FIGURE 14. The testing setup in experiments.

develop the dart score recognition for real-time implementation using openCV environment [21]. The processing time that includes the video sampling time, the recognition time, and the displaying result time, is requested within 3 seconds per shooting to meet real-time requirement for the practical blowgun system.

The recognition accuracy is affected under many factors, such as illumination change, target paper wobble, the camera setup direction deviation, and the dart overlapping problems. To overcome these problems, the initial calibration is proposed. Our system first calibrates the parameters according to the current testing situations. The maximum object tracking method can further reduce the affection of illumination changes and targets wobbles. The accuracy is dependent on the detection of dark tip. The dart tip is accurately detected by temporal segmentation and directional histogram approaches. By the references of calibrated points, the score of the dart tip can be estimated with high accuracy. The game rule is to shoot the five darts for one player. The current dart is possibly overlapped with the previous darts. The error detection will be increased in such a case. Hence we presented two cameras imaging system to improve the accuracy efficiently. The two cameras sampling would have binocular matching problem. In normal cases, the results of two cameras are the same. However, if one dart in a camera is overlapped with the previous ones, its score possibly is down. The other one camera samples the dart from the inverse direction, which may be no overlapped. The score is normal, which is higher than the result of the camera with dart overlapped. To solve the overlapping problem, we take the maximum score of the calculation from two cameras for the final score. However, when the dart is overlapped from both of two cameras, the results may be error, but this probability is quite low.

#### A. PRACTICAL DEMONSTRATION

The four windows are created with openCV. The left-up and right-up window is the sampling image of the left and right camera respectively. The left-bottom and right-bottom window is the estimated score for the current dart and the accumulation of the previous scores. Figure 15 (a)~(e) shows

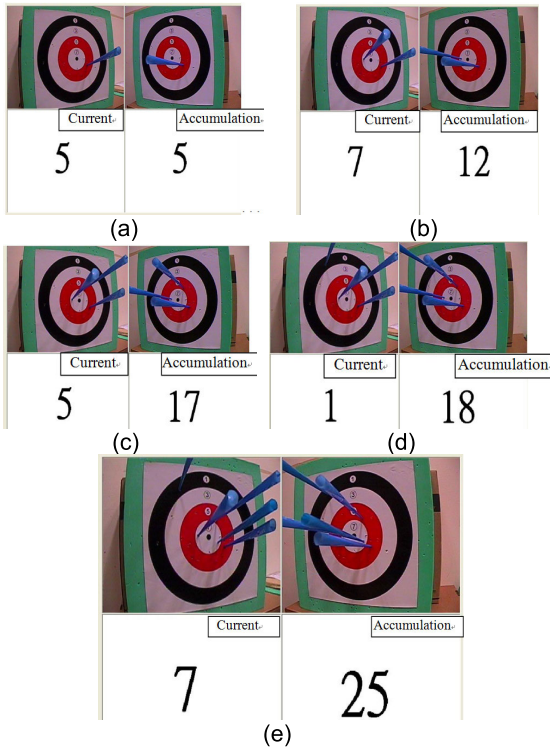


FIGURE 15. (a)~(e) testing results for the 1<sup>st</sup> ~5<sup>th</sup> darts, respectively.

the testing results of our automatic score recognition system. Figure 15(a) is the first shoot. The left-up and right-up image is sampled from the left and right camera respectively. The first dart score is five in both of the two cameras. The processing time is only about 0.35 sec per frame, which can meet the real-time requirement. Next, the second dart is shot, as shown in Fig. 15(b). Since the right-side camera appears two darts overlapping, the score may be wrong. The left camera samples two darts independently, and its score recognition is correct. When the darts are overlapping, its tip may be blanking and its recognition score becomes smaller. The maximum score is selected from the results of two camera recognition. The left bottom window shows that the score is seven for the second dart. The accumulation of the first and second darts score is 12, as shown in the bottom-right window. Next, the third, fourth and fifth dart, are shot, as shown in Fig. 15(c)-(e) respectively. The results are all correct. The real-time demonstration can refer to [22], where the lighting is flicker because of using fluorescent lamp. Results show that all scores are correct. Clearly, our algorithm can be against from the lighting change. By human recording method, the arguments are inevitable when the dart tip locates at the margin between two scores. Figure 16 shows the argument at the margin between score 5 and 7. The computer vision can make a fair judgment to avoid unnecessary argument. In our algorithm, when the tip is at the margin, the maximum score is found. In Fig. 16, the result is 7 when the tip is at the circle margin of the scores 5 and 7

To verify the accuracy of recognition, five peoples each shot 600 times randomly. The recognized score from the

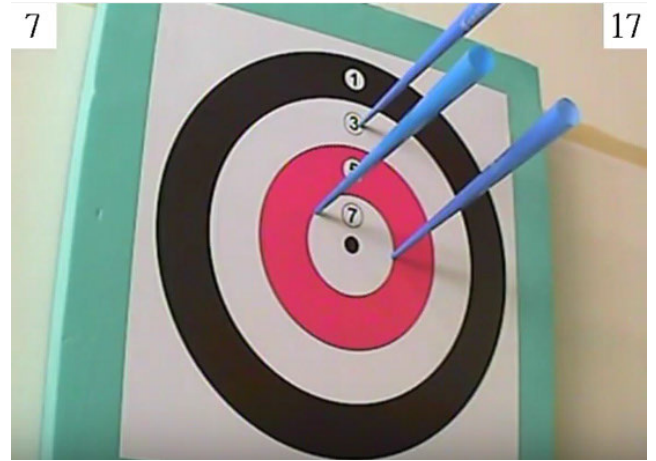


FIGURE 16. The argument at the margin between score 5 and 7.

TABLE 1. The recognition rate under various testers.

	Tester 1	Tester 2	Tester 3	Tester 4	Tester 5
Correct	582	590	578	581	585
Error	14	8	18	14	12
Lost	4	2	4	5	3
Accuracy	97.0%	98.3%	96.3%	96.8%	97.5%

computer is checked whether is correct. Table 1 shows the testing results, where “Correct” is that the recognition score meets to the practical score; “Error” denotes that the result is different from the practical dart score; “Lost” means that the system cannot detect the dart information. When five darts on the target are overlapping and crowding together, the score may be error, even lost the dart detection. If two darts are almost overlapped, the computer will miss the dart information since the two sampling patterns are very close. The missing case can be efficiently solved by using two cameras under inverse viewing angles. The accuracy can achieve about 97% on average, as listed in Table 1. The speed of recognition from the user shooting to display the score on the monitor is less than one second, which can meet real-time applications when the computer used Pentium CPU 3GHz, RAM 2G. This automatic scoring system can be used for blowgun games with high accuracy recognition.

### B. COMPLEXITY ANALYSIS FOR REAL-TIME SYSTEM

Now, the computational complexity of the proposed algorithm is analyzed for real-time operation. Since the computation complexity of subtraction is the same as addition, the additions are used instead of subtractions. For calibration step, the Sobel filter used 12 additions for horizontal and vertical direction for each pixel filtering. The maximum and minimum coordinates of cycles is searched by one passing comparison, hence required one comparison for per pixel. In order to reduce complexity, the distance computation in (1) used the absolute approach rather than root-square. 32 radiuses must be calculated, which requires  $32 \times 3$  additions and using 32 memory arrays to store the coordinates. In the calibration step,  $12(M \times N) + 96$  additions and  $M \times N - 1$



**TABLE 2. The computational complexity analysis of the proposed algorithm for per frame.**

	Cabiration Core	Recognition Core
Addition	12(MxN)+96	4(MxN)+98
Multiplication	0	2
Division	0	1
Comparison	MxN-1	33

**TABLE 3. Comparisons with competing algorithms.**

	[28]	[29]	[30]	Proposed
Target	Bullet	Darts	Archery	Blow Gun
Sensor	Piezoelectric Vibration	1 Camera	2 Cameras	2 Cameras
Application	Outdoor	Wide	Outdoor	Indoor
Lighting Effect	No	Serious	Middle	Little
Wobble Effect	Little	Serious	Serious	Little
Method	WiFi Sensor	Slope Detection	Ellipse Fitting	Distance Weighting
AccuracyRate	83~98%	75-80%	88~94%	96~98 %
Overlapping Solution	-	No	Yes	Yes
Calbration	No	No	Yes	Yes
Robustness	High	Low	Low	High

comparisons are required for per frame processing, where  $M \times N$  is the frame size. For the recognition step, the differential computing used one addition and the counter also used one addition for each pixel. A comparison is used to check dart appeared at the end of frame. Two counters are used to check the dart direction, which requires two additions per pixel. The dart position is calculated by 32 references using (3) by absolute approach, so this requires  $32 \times 3$  additions and 32 comparisons. Finally, ESD in (4) used two additions, two multiplications and one division. However, for ESD computing, we first search the minimum D1 and D2 from 32 references, so 32 comparisons are required. In the recognition core, the total number of additions and comparisons is  $4(M \times N) + 98$  and 33 respectively. Table 2 lists the computational complexity of our algorithm. Since the mathematic arithmetic is not too complex, the real-time work can be achieve using software implementation on a computer. The system can achieve about 3~5 frames per second (fps) for real-time score recognition, which can meet practical applications.

### C. COMPARISONS

Table 3 lists the comparisons with the competing techniques about the automatic scoring systems. The mechanical design of the automatic target-box with motor and gear assembly, consisting of target sheet, bullet-impact sensor, control board, and WiFi communication module was presented for bullet detection [28]. The implementation cost is very high. Instead, the low-cost scoring systems with computer vision were presented in [29], [30]. The darts on steel dartboard are detected using a standard webcam [29], which the rectilinear field of the dartboard are separated with line slopes mathematically. This method does not calibrate the parameters according to

the practical environment, the accuracy is not high. The stereo cameras for scoring system were presented in [30], which the ellipse fitting method used to mask the interested region on the targets to recognize the archery scores. They employ the models of ellipse to match the various circle size, which the computational complexity is very high. The computer vision methods face the problem of lighting change, which possibly effect the detection of dart segmentation and the scoring rings. In this study, to reduce the computational time for real-time purpose, the edge detection matching consisting of the color changes is used to find the boundary of each circle accurately, which the complexity is much lower than that of ellipse models. Our system calibrates the parameters for per player shooting while changes the target paper, which can promote the system robustness for the problems of the illumination change, target wobble, the camera setup direction change. The maximum object tracking can further reduce the affection of camera noise, and paper wobble on dart-impacting target. The testing accuracy and robutness can be efficiently improved on various environments. The current dart is possibly overlapped with the previous darts. The darts overlapping problem is solved by using two cameras imaging method, which can efficiently pomote the recognition rate. The proposed distance weighting method can calculate the score exactly.

### V. CONCLUSION

In this study, image processing techniques are presented to implement the automatic score recognition system. The worthwhile of this system is to record the scoring data to database automatically and to save the human power. The results can be shown on the display immediately for the score of the current dart and the accumulation of the previous ones. This can help the player to know his scores immediately. Besides, the system can avoid human error at the margin score to reduce unnecessary argument. Double cameras are presented to correct the viewing angles and also to reduce overlapping errors. The target paper can be automatically located by circle detection, and the center point can be quickly detected by the directional crossing approach. The initial calibration is proposed to overcome the deviation of viewing angles and reduce the affection on lighting changes. The dart tip can be detected and segmented accurately based on the hybrid computations of spatial and temporal processing. The weighted distance referred to calibrated points is proposed to calculate the dart score precisely. This system is successfully implemented to recognize the score of blowguns system in real-time applications. In future, by similar techniques, this system can be expanded to recognize archery and bullet scoring systems.

### REFERENCES

- [1] J. Chen, F. Shen, D. Z. Chen, and P. J. Flynn, "Iris recognition based on human-interpretable features," *IEEE Trans. Inf. Forensics Security*, vol. 11, no. 7, pp. 1476–1485, Jul. 2016.
- [2] Z. An, W. Deng, J. Hu, Y. Zhong, and Y. Zhao, "APA: Adaptive pose alignment for pose-invariant face recognition," *IEEE Access*, vol. 7, pp. 14653–14670, 2019.

- [3] F. Liu, D. Gu, and C. Chen, "IoU-related arbitrary shape text scoring detector," *IEEE Access*, vol. 7, pp. 180428–180437, 2019.
- [4] L. Jianfei, J. Wei, and G. Yuanhao, "Study on application of image recognition technique in the cow body condition score," in *Proc. IEEE 13th Int. Conf. Commun. Technol.*, Sep. 2011, pp. 373–376.
- [5] J. Guo, R. You, and L. Huang, "Mixed vertical-and-horizontal-text traffic sign detection and recognition for street-level scene," *IEEE Access*, vol. 8, pp. 69413–69425, 2020.
- [6] A. H. Ashtari, M. J. Nordin, and M. Fathy, "An iranian license plate recognition system based on color features," *IEEE Trans. Intell. Transp. Syst.*, vol. 15, no. 4, pp. 1690–1705, Aug. 2014.
- [7] L. Xie, T. Ahmad, L. Jin, Y. Liu, and S. Zhang, "A new CNN-based method for multi-directional car license plate detection," *IEEE Trans. Intell. Transp.*, vol. 19, no. 2, pp. 507–517, Feb. 2018.
- [8] H. Y. Lai and H. J. Lai, "Real-time dynamic hand gesture recognition," in *Proc. Int. Symp. Comput., Consum. Control*, Jun. 2014, pp. 658–661.
- [9] Sport Fukiya Association. Accessed: Oct. 12, 2020. [Online]. Available: <http://www.fukiya.net/>
- [10] A. Kanj, H. Talbot, J.-C. Pesquet, and R. R. Luparello, "Color deflickering for high-speed video in the presence of artificial lighting," in *Proc. IEEE Int. Conf. Image Process. (ICIP)*, Sep. 2015, pp. 976–980.
- [11] R. C. Bilcu, "Multiframe auto white balance," *IEEE Signal Process. Lett.*, vol. 18, no. 3, pp. 165–168, Mar. 2011.
- [12] R. C. Gonzalez and R. E. Woods, *Digital Image Processing*. Reading, MA, USA: Addison-Wesley, 1992.
- [13] X. Chen, L. Lu, and Y. Gao, "A new concentric circle detection method based on Hough transform," in *Proc. 7th Int. Conf. Comput. Sci. Educ. (ICCSE)*, Jul. 2012, pp. 753–758.
- [14] A. López and F. J. Cuevas, "Automatic multi-circle detection on images using the teaching learning based optimisation algorithm," *IET Comput. Vis.*, vol. 12, no. 8, pp. 1188–1199, Dec. 2018.
- [15] D. Wang, J. Yin, C. Tang, X. Cheng, and B. Ge, "Color edge detection using the normalization anisotropic Gaussian kernel and multichannel fusion," *IEEE Access*, vol. 8, pp. 228277–228288, 2020.
- [16] M. Mittal, A. Verma, I. Kaur, B. Kaur, M. Sharma, L. M. Goyal, S. Roy, and T.-H. Kim, "An efficient edge detection approach to provide better edge connectivity for image analysis," *IEEE Access*, vol. 7, pp. 33240–33255, 2019.
- [17] D. J. Bora, "An optimal color image edge detection approach," in *Proc. Int. Conf. Trends Electron. Informat. (ICEI)*, May 2017, pp. 342–347.
- [18] D. Zeng, X. Chen, M. Zhu, M. Goesele, and A. Kuijper, "Background subtraction with real-time semantic segmentation," *IEEE Access*, vol. 7, pp. 153869–153884, 2019.
- [19] K. Li, W. Tao, and L. Liu, "Online semantic object segmentation for vision robot collected video," *IEEE Access*, vol. 7, pp. 107602–107615, 2019.
- [20] Accessed: Dec. 11, 2019. [Online]. Available: <http://www.advantech.tw/default.aspx>
- [21] [Online]. Available: <https://opencv.org/releases/>
- [22] [Online]. Available: <http://www.youtube.com/watch?v=6uVeeNCMIkc>
- [23] C. Ye and H. Mi, "The technology of image processing used in automatic target-scoring system," in *Proc. 4th Int. Joint Conf. Comput. Sci. Optim.*, Apr. 2011, pp. 249–352.
- [24] K. Shiiya, T. T. Zin, M. Jomoto, and H. Watanabe, "A study on automatic display system of the archery score for the visually impaired," in *Proc. IEEE 6th Global Conf. Consum. Electron. (GCCE)*, Oct. 2017, doi: [10.1109/GCCE.2017.8229425](https://doi.org/10.1109/GCCE.2017.8229425).
- [25] Z. Su and W. Chen, "Effective target extraction of automatic target-scoring system," in *Proc. IEEE 4th Adv. Inf. Technol., Electron. Autom. Control Conf. (IAEAC)*, Dec. 2019, pp. 1402–1406.
- [26] P. R. Aryan, "Vision based automatic target scoring system for mobile shooting range," in *Proc. Int. Conf. Adv. Comput. Sci. Inf. Syst. (ICACSIS)*, 2012, pp. 325–329.
- [27] T. T. Zin, I. Oka, T. Sasayama, and S. Ata, "Image processing approach to automatic scoring system for archery targets," in *Proc. Int. Conf. Intell. Inf. Hiding Multimedia Signal Process.*, 2013, pp. 259–262.
- [28] I. Jattala, "Wireless sensor network (WSN) based automatic firing practice system (AFPS) for training of law enforcement agencies (LEAS)," *Int. J. Digit. Inf. Wireless Commun.*, vol. 4, no. 4, pp. 408–417, 2014.
- [29] S. Hensel, M. B. Marinov, F. Sprich, and B. Ganey, "Image-based automated hit detection and score calculation on a steel dartboard," in *Proc. 2nd Balkan Junior Conf. Lighting (Balkan Light Junior)*, Sep. 2019, doi: [10.1109/BLJ.2019.8883659](https://doi.org/10.1109/BLJ.2019.8883659).
- [30] L. A. Danielescu, "On target: An electronic archery scoring system," AX, Phoenix, AZ, USA, Tech. Rep., 2007.



**SHIH-CHANG HSIA** received the Ph.D. degree from the Department of Electrical Engineering, National Cheng Kung University, Tainan, Taiwan, in 1996. From 1986 to 1989, he was an Engineer with the Research and Development Department, Microtek International Inc., Hsinchu. From 1991 to 1998, he was an Instructor and an Associate Professor with the Department of Electronics Engineering, Chung Chou Institute of Technology. From 1998 to 2010, he was a Professor with the Department of Computer and Communication Engineering, and the Department of Electronic Engineering, National Kaohsiung University of Science and Technology Kaohsiung. He was elected as the Chairman of the Department of Electronics Engineering, from 2007 to 2009. He is currently a Professor with the Department of Electronics Engineering, National Yunlin University of Science and Technology. His research interests include VLSI/SOC designs, video/image coding and processing, neural network design and its application, smart lighting system and electrical sensors, and micro-LED display.



**SZU-HONG WANG** was born in Yunlin, Taiwan. He received the B.S. degree from the Department of Computer and Communication Engineering, National Kaohsiung University of Science and Technology, Kaohsiung, Taiwan, in 2005, and the Ph.D. degree from the Institute of Engineering Science and Technology, National Kaohsiung First University of Science and Technology, in 2010. He is currently an Associate Professor with the Bachelor Program in Interdisciplinary Studies, National Yunlin University of Science and Technology. His main research interests include neural networks, image processing, DSP/VLSI architecture design, and embedded systems.

**WEI-CHUN CHENG** received the M.S. degree in electrical engineering from the National Yunlin University of Science and Technology, Yunlin, Taiwan, in 2012. His main research interests include image processing and embedded systems.



**CHUAN-YU CHANG** (Senior Member, IEEE) received the M.S. degree in electrical engineering from National Taiwan Ocean University, Keelung, Taiwan, in 1995, and the Ph.D. degree in electrical engineering from National Cheng Kung University, Tainan, Taiwan, in 2000. From 2001 to 2002, he was with the Department of Computer Science and Information Engineering, Shu-Te University, Kaohsiung, Taiwan. From 2002 to 2006, he was with the Department of Electronic Engineering,

National Yunlin University of Science and Technology, Yunlin, Taiwan, where he has been with the Department of Computer and Communication Engineering. His current research interests include neural networks and their application to medical image processing, wafer defect inspection, digital watermarking, and pattern recognition. In the above areas, he has authored or coauthored more than 150 publications in journal articles and conference proceedings. He is the Chair of the IEEE Signal Processing Society Tainan Chapter.

• • •